International Journal of Automotive Technology, Vol. 6, No. 3, pp. 293–303 (2005)

1229-9138/2005/021-13

EFFECTS OF INTERFACE CRACKS EMANATING FROM A CIRCULAR HOLE ON STRESS INTENSITY FACTORS IN BONDED DISSIMILAR MATERIALS

N.-Y. CHUNG[1)*] and C.-H. SONG[2)]

[1)]Department of Mechanical Engineering, Soongsil University, Seoul 156-743, Korea
[2)]AMLCD Division, Samsung Electronics Co., Ltd., Yongin-si, Gyeonggi 449-711, Korea

(Received 19 December 2004; Revised 14 January 2004)

ABSTRACT– Bonded dissimilar materials are being increasingly used in automobiles, aircraft, rolling stocks, electronic devices and engineering structures. Bonded dissimilar materials have several material advantages over homogeneous materials such as high strength, high reliability, light weight and vibration reduction. Due to their increased use it is necessary to understand how these materials behave under stress conditions. One important area is the analysis of the stress intensity factors for interface cracks emanating from circular holes in bonded dissimilar materials. In this study, the bonded scarf joint is selected for analysis using a model which has comprehensive mixed-mode components. The stress intensity factors were determined by using the boundary element method (BEM) on the interface cracks. Variations of scarf angles and crack lengths emanating from a centered circular hole and an edged semicircular hole in the Al/Epoxy bonded scarf joints of dissimilar materials are computed. From these results, the stress intensity factor calculations are verified. In addition, the relationship between scarf angle variation and the effect by crack length and holes are discussed.

KEY WORDS : Bonded dissimilar materials, Interface crack, Bonded scarf joint, Centered circular hole, Edged semicircular hole, Stress intensity factor, Boundary element method

1. INTRODUCTION

The application of bonded dissimilar materials for light weight, high strength, high reliability and special purposes is increasing in various industries such as ceramics/metal and resin/metal bonded joints, IC packages, beam welding and friction welding, brazing, coating, and soldering techniques. Bonded dissimilar materials, used in automobiles, rolling stocks, aircraft, electronic devices and engineering structures, have various advantages over other materials in terms of material properties, absorption of vibration and impact, and buffer and fatigue endurance.

Though bonded dissimilar materials have a wide range of applications, little research has been conducted on the strength evaluation of the interface crack in these materials. A high precision analysis of stress and calculation of fracture parameters using the analyzed stress results should be conducted before the establishment of fracture criteria.

In order to establish the fracture criterion, modeling of a simple specimen which can obtain comprehensive mixed-mode conditions for bonded structures of dissimilar materials is needed. In this study, the bonded scarf joint is selected for the analysis model which has comprehensive mixed-mode components.

The interface crack initiates at the interface edge, where the stress concentration is greatest. The crack propagates from the interface edge and it always occurs by mixed-mode along the interface (Chung, 1996; Chung, 1997).

However, the presence of microscopic flaws such as voids and blow holes, and macroscopic flaws such as notches and inclusions, or circular holes and elliptical holes can accelerate the initiation and propagation of the edged interface crack.

It is very important to analyze stress intensity factors for interface cracks emanating from holes in bonded dissimilar materials. Since cracks generally originate at a circular hole in structures, it is necessary that the effect of a hole should be included in the calculation of stress intensity factors (Murakami, 1982; Kuo, 1983; Salama, 1996).

Bowie (Bowie, 1956) solved the problems for cracks originating from a circular hole by the conformal mapping method in a homogeneous material. Newman

*Corresponding author. e-mail: nychung@hanmail.net

(Newman, 1971) employed the boundary collocation method and analyzed the same problem both for the finite and infinite plates. Woo *et al.* (Woo, 1989) analyzed the mixed-mode stress intensity factors of two inclined cracks emanating from a hole in a finite plate by Muskhelishivili formulation and the boundary collocation method.

Interface cracks appear to have been first studied by Williams (Williams, 1959) and Erdogan (Erdogan, 1963), who found the stresses around a crack on an interface between two isotropic elastic bodies under conditions of plane strain. Further results for this problem were given by England (England, 1965), Erdogan (Erdogan, 1965) and Rice and Sih (Rice, 1965).

In addition, a crack on an interface between isotropic plates under conditions of plane stress was studied by Groth (Groth, 1967). Comninou (Comninou, 1977) resolved the problems at the crack tip by solving the interfacial crack problem assuming there is a small contact zone near the crack tips. He and Hutchinson (He, 1989) performed an analysis very similar to the present one for the case of a branched semi-infinite crack. Rice (Rice, 1988) and Yuuki *et al.* (Yuuki, 1989) proposed a method to determine the stress intensity factors of an interface crack. They calculated the stress intensity factors for an interface crack by the boundary element method(BEM) using Hetenyi's fundamental solution for dissimilar materials.

The two-dimensional problem of a crack along an interface between two different isotropic elastic solids has been studied by Chung (Chung *et al.*, 2000; Chung, 2002; Chung and Park, 2004), and an extensive list of references is found in a paper by Mukai *et al.* (Mukai, 1990). These studies analyzed the energy release rate of a finite length crack branching off from the interface between two bonded isotropic materials.

However, the stress intensity factors of slant interface cracks emanating from a circular hole in dissimilar materials has not been analyzed yet. In this study, we assume that the circular hole idealized microscopic and macroscopic defects, and the analysis models with the edged interface crack and interface crack emanating from edged semicircular holes in the bonded scarf joints of dissimilar materials were selected. In order to investigate the precision of the analysis and the variations in the stress intensity factors on the slant interfacial crack emanating from a centered circular hole and the edged semicircular hole in bonded scarf joints, we have analyzed both simultaneously by using the boundary element method.

In this paper, therefore, the stress intensity factors of the interface crack for various scarf angles, crack lengths and hole radii in the Al/Epoxy bonded joints of dissimilar materials were analyzed by using the boundary element method, and the relationships and validities of these stress intensity factors were investigated.

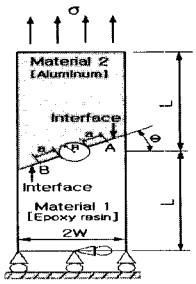

(a) Interface crack emanating from a circular hole

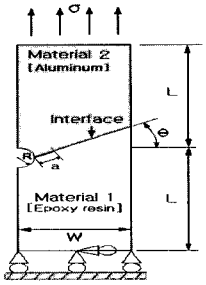

(b) Interface crack emanating from an edged semicircular hole

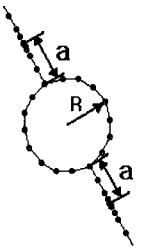

(c) Element mesh pattern around a circular hole and interface crack

Figure 1. Model of a slant interfacial crack emanating from a hole in bonded dissimilar materials.

2. STRESS ANALYSIS OF INTERFACE CRACKS BY BEM

2.1. Analysis Models of Interface Cracks

Models and constraint conditions to calculate the stress intensity factors by using BEM for the interface cracks emanating from a circular hole are shown in Figure 1. In Figure 1, material 1 is epoxy resin and material 2 is aluminum alloy. Numerical analysis is performed by using BEM and varying the radius of a circular hole, crack length, and slant angle. In Figure 1, the radius of a circular hole is r, the crack length is a, the slant angle is θ, the width of specimen (W) is 30 mm, and the length of the specimen (L) is 60 mm.

The slant interfacial crack emanating from a centered

circular hole is shown in Figure 1(a) and that from an edged semicircular hole in Figure 1(b). Figure 1(c) depicts the element mesh pattern around a circular hole and interface crack for BEM analysis.

2.2. Interface Crack-tip Stress Field

The interface crack-tip stress field of bonded dissimilar materials with boundary conditions where traction is free in Figure 2 can be expressed as the following equations.

$$\sigma_{ij} = \frac{1}{\sqrt{r}}A_{ij}(\theta)\sin\left(\varepsilon\ln\frac{r}{l}\right)+\frac{1}{\sqrt{r}}B_{ij}(\theta)\cos\left(\varepsilon\ln\frac{r}{l}\right) \quad (1)$$

$$\varepsilon = \frac{1}{2\pi}\ln\left[\left(\frac{k_1}{\mu_1}+\frac{1}{\mu_2}\right)/\left(\frac{k_2}{\mu_2}+\frac{1}{\mu_1}\right)\right] \quad (2)$$

$$k_j = \begin{cases} 3-4\nu_j & (plane\ strain) \\ \dfrac{3-\nu_j}{1+\nu_j} & (plane\ stress)\ (j=1,2) \end{cases} \quad (3)$$

where ε is the constant of dissimilar materials, μ is the shear modulus, and ν is the Poisson's ratio. In addition, r is the distance from the crack tip, and l is the reference length of the crack. It has been reported that the oscillating singularity occurs very close to the crack tip (Yuuki, 1989). Note that the oscillating singularity occuring at the crack tip is expressed in equation (1) and because this oscillating singularity occurs very close to the crack-tip, it could be ignored.

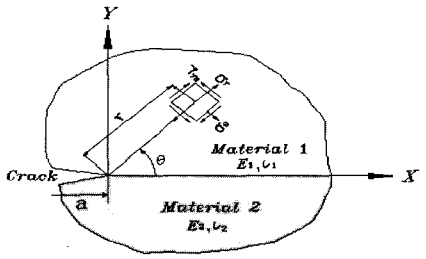

Figure 2. Crack-tip stress field in the bonded dissimilar materials.

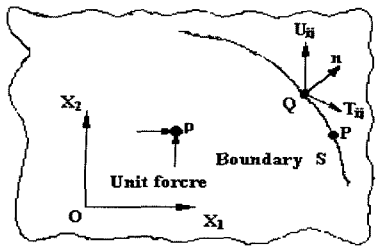

Figure 3. Unit force acting on a point of infinite plate.

2.3. Fundamental Solutions

When a unit force is applied at p in the i-direction of an infinite plate as shown in Figure 3, U_{ij} and T_{ij} are fundamental solutions at Q in the j-direction. This means the traction and displacement respectively at Q in the j-direction are due to a unit force at P in the i-direction. For two-dimensional isotropic elasticity, the U_{ij} and T_{ij} defined in equations (4) and (5) are well known as the Kelvin's solutions in plane strain condition (Kane, 1994).

$$U_{ij}(P,Q) = \frac{1}{8\pi(1-\upsilon)\mu}\left[(3-4\upsilon)\log\left(\frac{1}{r}\right)\delta_{ij}+r,_i r,_j\right] \quad (4)$$

$$T_{ij}(P,Q) = -\frac{1}{4\pi(1-\upsilon)}\left[\{(1-2\upsilon)\delta_{ij}+2r,_i r,_j\}\frac{\partial r}{\partial n} -(1-2\upsilon)(r,_i n_j - r,_j n_i)\right] \quad (5)$$

where δ_{ij} is the Kronecker delta, and n is the unit outward normal vector. For the case of plane stress conditions, $\nu'=\nu/(1+\nu)$ is substituted for ν in the above equations.

In addition, r, $r,_i$ and r/n in equations (4) and (5) are defined as in the following equations:

$$\begin{aligned} r &= PQ = \sqrt{r_i r,_i}, r_i = x_i(Q)-x_i(P) \\ r,_j &= \left.\frac{\partial r}{\partial x_i}\right|_Q = \frac{r_i}{r} \\ \frac{\partial r}{\partial n} &= \frac{\partial r}{\partial x_1}\frac{\partial x_1}{\partial n}+\frac{\partial r}{\partial x_2}\frac{\partial x_2}{\partial n} \end{aligned} \quad (6)$$

$$U_{ij}(P,Q) = \frac{1}{16\pi(1-\upsilon)\mu r}\{(3-4\upsilon)\delta_{ij}+r,_i r,_j\} \quad (7)$$

$$T_{ij}(P,Q) = \frac{1}{8\pi(1-\upsilon)r^2}\left[\{(1-2\upsilon)\delta_{ij}+3r,_i r,_j\}\frac{\partial r}{\partial n} -(1-2\upsilon)(r,_i n,_j - r,_j n,_i)\right] \quad (8)$$

2.4. Stress Intensity Factors for the Interface Crack

After the stresses of interface cracks are analyzed by BEM, the fracture mechanic parameters for an interface crack in bonded dissimilar materials can be calculated. Stress intensity factors can be obtained by extrapolation as in the following equations (Chung, 1996).

$$K_1 = \lim_{r\to 0}\sqrt{2\pi r}(\sigma_y cos\theta+\tau_{xy}sin\theta) \quad (9)$$

$$K_2 = \lim_{r\to 0}\sqrt{2\pi r}(\tau_{xy}sin\theta+\sigma_y sin\theta) \quad (10)$$

$$F_1 = K_1/\sigma\sqrt{\pi l} \quad (11)$$

$$F_2 = K_2/\sigma\sqrt{\pi l} \quad (12)$$

$$Q = \varepsilon \ln(r/l) \quad (13)$$

where K_1 and K_2 are complex stress intensity factors, and F_1 and F_2 are normalized stress intensity factors for an interface crack, l is the reference crack length, a denotes an edge crack, and $2a$ denotes a center crack.

3. RESULTS AND DISCUSSION

3.1. Verification of the Analysis Results

To analyze stress using BEM for models, they are divided into two areas and the number of total elements is 284. Mechanical properties of materials listed in Table 1 were measured directly in the experiments.

After the stress analysis was performed for the models shown in Figure 1 using the mechanical properties of the materials of Table 1, stress intensity factors were computed at crack-tips A and B by using Kelvin's solution, 2-dimensional elastic analysis and singular elements, which resulted in high precision.

Table 2 compares the stress intensity factors determined by Freese (Bowie, 1973) and by BEM at two slant angles (θ=30° and 45° to the interfacial edge cracks) for four a/W ratios in a homogeneous material with the theoretical solutions (Isida, 1984). The results were estimated to be accurate within 0.1%.

Table 3 compares the analytical and numerical solution of stress intensity factors determined by Raju (Raju, 1987) and those we determined by BEM for interfacial center cracks under plane strain conditions in bonded dissimilar materials. These results agree with our results within 0.03%.

Table 1. Mechanical properties of materials.

Mechanical properties / Materials	Young's modulus E(GPa)	Poisson's ratio ν
Epoxy resin	3.175	0.37
Aluminum	65.56	0.32

Table 2. Stress intensity factors of interfacial edge cracks.

θ	30		45	
F	F_1		F_1	
a/W	Freese	BEM (Our)	Freese	BEM (Our)
0.2	1.11	1.120	0.80	0.797
0.3	1.28	1.270	0.90	0.898
0.4	1.55	1.551	1.02	1.031
0.5	1.98	1.964	1.27	1.275

Table 3. Stress intensity factor of a center crack in bonded dissimilar materials.

Methods \ Materials	Steel/Al	Al/Epoxy	Steel/Epoxy
	F	F	F
Analytical	1.0040	1.0090	1.0100
BEM (Our)	1.0038	1.0092	1.0097
BEM (Yuuki)	1.0040	1.0080	1.0090
FEM (Raju)	0.9790	1.0160	1.0160

3.2. Results of Interface Cracks Emanating from a Centered Circular Hole

3.2.1. Case of fixed hole radius and varied crack length

The stress intensity factors determined by BEM for interfacial crack-tip A and B of Al/Epoxy bonded dissimilar materials as shown in Figure 1(a), are listed in Table 4. The stress intensity factors in Table 4 are for interface cracks emanating from a circular hole with a radius of 5 mm (R/W=0.167) at various slant angles (θ= 0°, 15°, 30°, 45°, 60°), crack lengths (a=0.1 mm, 0.5 mm, 1 mm, 3 mm, 6 mm, 9 mm, 12 mm and 15 mm), and a/W ratios (a/W=0.003, 0.017, 0.033, 0.1, 0.2, 0.3, 0.4, 0.5).

Figure 4 shows the variations of crack lengths for slant angle and the results of stress intensity factors, F_1 and F_2, for the crack-tip A as listed in Table 4. As shown in Figure 4(a), F1A increases with increasing crack length over the entire range of a/W ratios. F_{1A} increases rapidly from a/W=0 to a/W=0.1. Thereafter, it increases gradually. As shown in Figure 4(b), F_{2A} increases rapidly with increasing of the crack length. The increase remains proportional below θ=45° and the increasing values vary with lower ranges in case of θ=60° than that of θ=45°.

Figure 5 shows the relationships between crack lengths and slant angles. Listed are the results of stress intensity factors F_1 and F_2 for crack-tip B in Table 5. In Figure 5(a), F_{1B} decreases in proportion to the growth of crack length from a/W=0 to a/W=0.1. Thereafter, it increases gradually over a/W=0.1, and decreases sharply with increasing slant angle. In Figure 5(b), F_{2B} increases rapidly with increasing crack length over the entire range of a/W ratios, but the values for θ=45° are higher than those of θ=60°. F1 and F2 are more strongly affected by crack length than those of holes when the crack lengths are short. Stress intensity factors for crack-tip B are affected strongly by crack length, so the values for crack-tip B are higher than those for crack-tip A.

3.2.2. Case of fixed crack length and varied hole radius

Table 5 shows the stress intensity factors determined by BEM for interface cracks in the analytical model for Al/Epoxy bonded dissimilar materials as shown in Figure 1(a). The stress intensity factors for crack- tips A and B

Table 4. Stress intensity factor of an interface crack emanating from a circular hole.

θ \ a/W	F	0.003	0.017	0.033	0.100	0.200	0.300	0.400	0.500
0°	$F_{1A,B}$	0.930	0.990	1.200	1.322	1.415	1.540	1.665	1.789
	$F_{2A,B}$	0.036	0.043	0.059	0.098	0.170	0.230	0.264	0.298
15°	F_{1A}	0.560	0.812	0.927	1.087	1.299	1.414	1.512	1.644
	F_{1B}	1.293	1.342	1.389	1.445	1.474	1.518	1.532	1.598
	F_{2A}	0.041	0.050	0.061	0.178	0.287	0.335	0.380	0.420
	F_{2B}	0.030	0.041	0.045	0.125	0.223	0.284	0.320	0.359
30°	F_{1A}	0.217	0.234	0.418	0.636	0.742	0.802	0.853	0.929
	F_{1B}	0.954	0.945	0.932	0.880	0.881	0.919	0.973	1.053
	F_{2A}	0.048	0.055	0.066	0.200	0.312	0.389	0.419	0.457
	F_{2B}	0.200	0.212	0.231	0.284	0.293	0.282	0.191	0.252
45°	F_{1A}	0.192	0.212	0.265	0.444	0.578	0.664	0.754	0.833
	F_{1B}	1.070	0.970	0.940	0.921	0.900	0.912	0.938	0.990
	F_{2A}	0.048	0.080	0.200	0.410	0.553	0.610	0.657	0.685
	F_{2B}	0.053	0.212	0.337	0.387	0.429	0.440	0.450	0.453
60°	F_{1A}	0.173	0.194	0.217	0.254	0.316	0.320	0.365	0.380
	F_{1B}	0.547	0.520	0.490	0.456	0.423	0.436	0.475	0.488
	F_{2A}	0.090	0.150	0.189	0.290	0.383	0.420	0.480	0.520
	F_{2B}	0.100	0.145	0.188	0.265	0.327	0.346	0.375	0.394

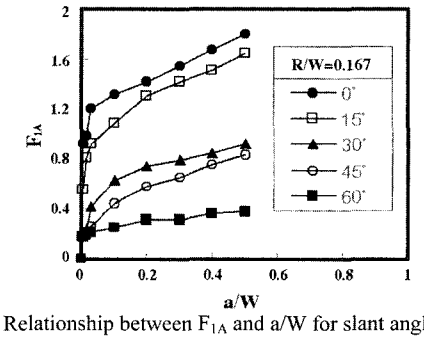

(a) Relationship between F_{1A} and a/W for slant angle

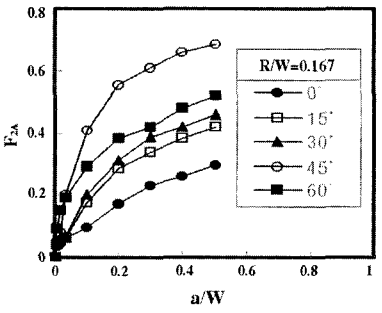

(b) Relationship between F_{2A} and a/W for slant angle

Figure 4. Stress intensity factor for interface crack-tip A emanating from a circular hole (R/W=0.167).

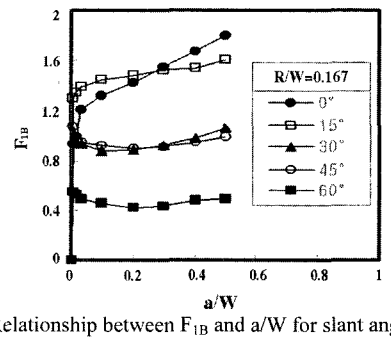

(a) Relationship between F_{1B} and a/W for slant angle

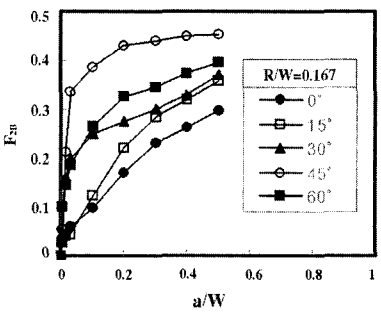

(b) Relationship between F_{2B} and a/W for slant angle

Figure 5. Stress intensity factor for interface crack-tip B emanating from a circular hole (R/W=0.167).

are shown in Figures 6 and 7 when the crack length a is fixed at 3 mm (a/W=0.1) at various slant angles (θ=0°, 15°, 30°, 45°, 60°), center circular hole radii (R=0.5 mm, 1 mm, 3 mm, 6 mm, 9 mm, 12 mm and 15 mm), and R/W ratios (R/W=0.00167, 0.03, 0.05, 0.1, 0.2, 0.3, 0.4, 0.5).

Figure 6 shows the F_{1A} and F_{2A} for crack-tip A at various R/W ratios and slant angles. Figure 6(a) shows that F_{1A} increases gradually with increasing hole radii and decreases rapidly with increasing slant angles. Also, as shown in Figure 6(b), F2A increases with increasing slant angles below θ=45° and hole radii from θ=0°~15°. However, F_{2A} increases rapidly as the hole radii was increased θ=30° to 45°. At slant angle of θ=60°, F_{2A} decreases more than it does at θ=30°.

Figure 7 shows F_{1B} and F_{2B} of the crack-tip B for various R/W ratios and slant angles. As shown in Figure 7(a), F_{1B} increases slightly with increasing hole radius when θ=0°, and it decreases gradually with increasing slant angle and hole radius, when θ=15°~60°. Fig. 7(b) depicts F_{2B} for various hole radii and slant angles. F_{2B} increases gradually with increasing slant angle by influence of the shear stress below θ=15° and decreases rapidly due to interference of the hole over θ=30°. The stress intensity factor is more strongly affected by the variation of hole radius for crack-tip B than that for

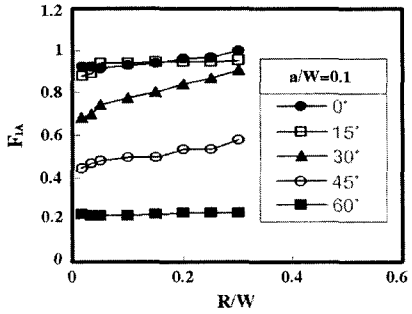

(a) Relationship between F_{1A} and R/W for slant angle

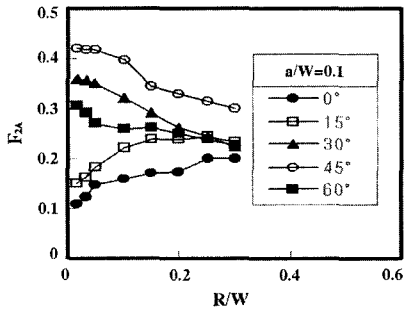

(b) Relationship between F_{2A} and R/W for slant angle

Figure 6. Stress intensity factor for interface crack-tip A emanating from a circular hole (a/W=0.1).

Table 5. Stress intensity factor of an interface crack emanating from a circular hole.

θ \ R/W	F	0.00167	0.03	0.05	0.10	0.20	0.30	0.40	0.50
0°	$F_{1A,B}$	0.92	0.92	0.92	0.93	0.94	0.96	0.97	0.99
	$F_{2A,B}$	0.11	0.12	0.15	0.16	0.17	0.17	0.19	0.20
15°	F_{1A}	0.88	0.89	0.94	0.94	0.95	0.95	0.95	0.95
	F_{1B}	0.80	0.80	0.80	0.79	0.79	0.79	0.78	0.76
	F_{2A}	0.15	0.16	0.18	0.22	0.24	0.24	0.24	0.23
	F_{2B}	0.35	0.39	0.40	0.49	0.37	0.36	0.36	0.35
30°	F_{1A}	0.68	0.69	0.74	0.77	0.81	0.84	0.87	0.91
	F_{1B}	0.63	0.62	0.62	0.60	0.59	0.56	0.53	0.53
	F_{2A}	0.36	0.32	0.35	0.32	0.29	0.26	0.24	0.22
	F_{2B}	0.52	0.52	0.52	0.49	0.46	0.44	0.42	0.42
45°	F_{1A}	0.44	0.47	0.48	0.49	0.49	0.53	0.54	0.58
	F_{1B}	0.41	0.41	0.40	0.38	0.35	0.33	0.32	0.32
	F_{2A}	0.42	0.42	0.42	0.39	0.34	0.33	0.32	0.30
	F_{2B}	0.54	0.51	0.51	0.48	0.44	0.40	0.37	0.36
60°	F_{1A}	0.23	0.22	0.22	0.22	0.23	0.23	0.23	0.23
	F_{1B}	0.19	0.19	0.19	0.17	0.13	0.11	0.08	0.07
	F_{2A}	0.31	0.29	0.27	0.26	0.26	0.25	0.24	0.23
	F_{2B}	0.34	0.35	0.34	0.31	0.28	0.26	0.24	0.22

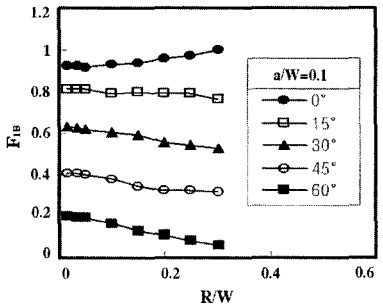

(a) Relationship between F_{1B} and R/W for slant angle

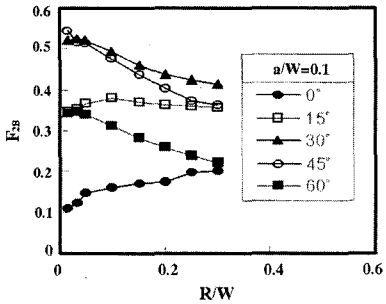

(b) Relationship between F_{2B} and R/W for slant angle

Figure 7. Stress intensity factor for interface crack-tip B emanating from a circular hole (a/W=0.1).

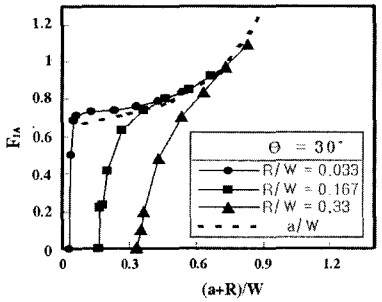

(a) Relationship between F_{1A} and (a+R)/W for R/W

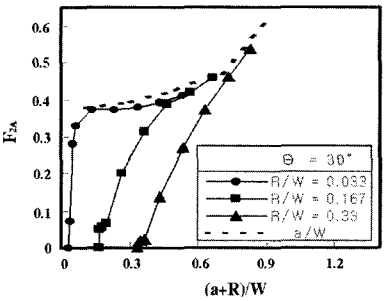

(b) Relationship between F_{2A} and (a+R)/W for R/W

Figure 8. Stress intensity factor for interface crack-tip A emanating from a circular hole (θ=30°).

crack-tip A. Therefore, F_{1B} and F_{2B} are more influenced to increasing hole size than F_{1A} and F_{2A}.

3.2.3. Case of simultaneously varied crack length and hole radius

Table 6 lists the results of stress intensity factors for interface cracks by BEM in the analytical model of Al/Epoxy bonded dissimilar materials as shown in Figure 1(a). Figures 8 and 9 show the stress intensity factors for crack-tips A and B are shown for a slant angle of θ=30° at various circular hole radii, crack lengths and a/W ratios.

Figure 8 shows the stress intensity factor for crack-tip A as listed in Table 6. As shown in Figure 8(a) and (b), F_{1A} and F_{2A} increase rapidly with increasing crack length

Table 6. Stress intensity factor of an interface crack emanating from a circular hole.

R \ a/W, F	F	0.003	0.017	0.033	0.100	0.200	0.300	0.400	0.500
1 mm	F_{1A}	0.506	0.685	0.715	0.735	0.739	0.739	0.790	0.835
	F_{1B}	0.878	0.829	0.805	0.793	0.820	0.856	0.896	0.949
	F_{2A}	0.072	0.282	0.329	0.372	0.372	0.379	0.394	0.414
	F_{2B}	0.050	0.060	0.082	0.092	0.120	0.160	0.228	0.294
5 mm	F_{1A}	0.217	0.234	0.418	0.636	0.742	0.802	0.853	0.929
	F_{1B}	0.954	0.945	0.932	0.880	0.881	0.919	0.973	1.053
	F_{2A}	0.048	0.055	0.066	0.200	0.312	0.389	0.419	0.457
	F_{2B}	0.200	0.210	0.230	0.280	0.290	0.280	0.190	0.250
10 mm	F_{1A}	0.005	0.100	0.199	0.484	0.705	0.836	0.975	1.099
	F_{1B}	0.939	1.015	0.020	0.013	0.010	0.054	1.148	1.249
	F_{2A}	0.010	0.020	0.023	0.140	0.270	0.373	0.462	0.539
	F_{2B}	0.045	0.140	0.180	0.290	0.360	0.420	0.490	0.604

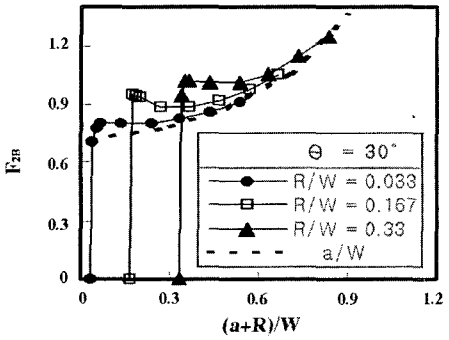

(a) Relationship between F_{1B} and (a+R)/W for R/W

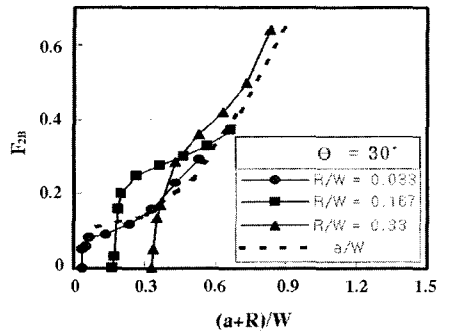

(b) Relationship between F_{2B} and (a+R)/W for R/W

Figure 9. Stress intensity factor for interface crack-tip B emanating from a circular hole (θ=30°).

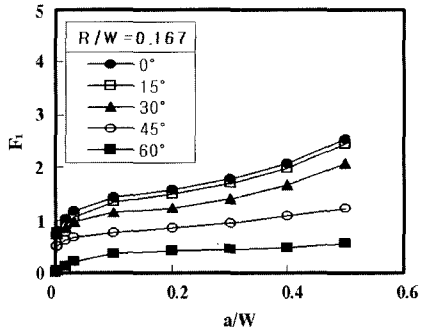

(a) Relationship between F_1 and a/W for slant angle

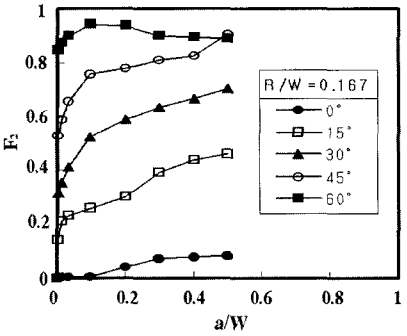

(b) Relationship between F_2 and a/W for slant angle

Figure 10. Stress intensity factor for interface crack emanating from an edged semicircular hole (R/W=0.167).

when R/W=0.167 and R/W=0.33. F_{1A} and F_{2A} increase rapidly with increasing crack length due to the influence of a hole when R/W=0.033 and a/W<0.1. F_{1A} and F_{2A} approach approximate values of the interfacial center cracks, which have no holes, without affecting the crack length when R/W=0.033 and a/W>0.1 when the crack length is larger than the hole radius. Therefore, when a/R>1, because F_{1A} and F_{2A} approach approximate values of the interfacial center cracks which have no holes, a center hole has little influence on the stress intensity factors. As the crack length reaches a certain value, the stress intensity factors with both cracks and holes converge to constant values which have only cracks, so holes have little influence on stress intensity factors when the crack lengths are over a certain value.

Figure 9 shows F_{1B} and F_{2B} for the crack-tip B as listed in Table 6. In Figure 9(a), F_{1B} increases gradually with increasing crack length, and it decreases due to the influence of the hole when R/W=0.167 and a/W<0.1. In Figure 9(b), F_{1B} increases because it has been influenced by cracks and holes. As previously mentioned, when the crack length reaches a certain value, the hole has little influence when crack lengths are over a certain value.

3.3. Results of Interface Cracks Emanating from an Edged Semicircular Hole

3.3.1. Case of fixed radius of an edged semicircular hole and varied crack length

For the analytical model of Al/Epoxy bonded dissimilar materials as shown in Figure 1(b), the values of F_1 and F_2 are listed in Table 7. In this figure, the stress intensity factors are calculated when the radius of a semicircular hole is R=5 mm and the crack lengths are a=3 mm, 6 mm, 9 mm, 12 mm and 15 mm (a/W=0.1, 0.2, 0.3, 0.4, 0.5).

Figure 10 shows the results of numerical analysis for various a/W ratios and slant angles. As shown in Figure 10(a), F_1 increases with increasing crack lengths and slant angles when θ=60°, and decreases gradually when a/W> 0.1.

3.3.2. Case of fixed crack length and varied radius of an edged semicircular hole

The F_1 and F_2 values for the analytical model of Al/Epoxy bonded dissimilar materials as shown in Figure 1(b) are listed in Table 8. The stress intensity factors shown in Figure 11 were calculated when the crack length is a=3 mm and the radii of semicircular holes are R=1.5 mm, 3 mm, 4.5 mm, 6 mm, 7.5 mm and 9 mm (R/W=0.05, 0.1, 0.15, 0.2, 0.25, 0.3).

In Figure 11(a), F1 increases with increasing hole radii but it decreases with increasing slant angle because of the

Table 7. Stress intensity factor of an interface crack emanating from an edged semicircular hole.

θ \ a/W, F		0.1	0.2	0.3	0.4	0.5
0°	F_1	1.412	1.577	1.768	2.050	2.530
	F_2	-0.0065	-0.042	-0.073	-0.077	-0.086
15°	F_1	1.334	1.496	1.680	1.965	2.454
	F_2	0.258	0.300	0.390	0.440	0.462
30°	F_1	1.123	1.216	1.383	1.644	2.050
	F_2	0.522	0.589	0.634	0.667	0.706
45°	F_1	0.756	0.836	0.923	1.066	1.216
	F_1	0.755	0.776	0.810	0.825	0.905
60°	F_2	0.404	0.415	0.427	0.465	0.555
	F_2	0.943	0.935	0.901	0.896	0.891

Table 8. Stress intensity factor of an interface crack emanating from an edged semicircular hole.

θ \ R/W, F		0.05	0.10	0.15	0.20	0.25	0.30
0°	F_1	1.32	1.34	1.39	1.46	1.53	1.61
	F_2	-0.032	-0.022	-0.008	-0.014	0.086	0.086
15°	F_1	0.237	0.308	1.368	1.394	1.497	1.535
	F_2	0.178	0.245	0.253	0.257	0.282	0.300
30°	F_1	1.06	1.07	1.12	1.18	1.26	1.32
	F_2	0.505	0.508	0.519	0.527	0.554	0.558
45°	F_1	0.724	0.749	0.787	0.830	0.894	0.977
	F_1	0.793	0.780	0.752	0.748	0.738	0.735
60°	F_2	0.406	0.405	0.438	0.425	0.515	0.570
	F_2	1.024	0.935	0.926	0.918	0.907	0.897

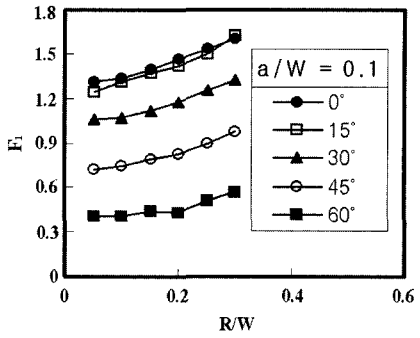

(a) Relationship between F_1 and R/W for slant angle

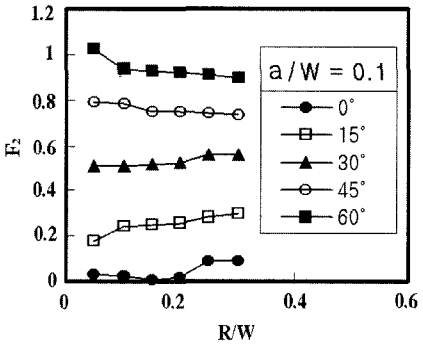

(b) Relationship between F_2 and a/W for slant angle

Figure 11. Stress intensity factor for an interface crack emanating from an edged semicircular hole (a/W=0.1).

influence of the edged semicircular hole.

Additionally, as shown in Figure 11(b), F2 increases with increasing slant angle and crack length when θ=30°, but it decreases with increasing crack length when θ=45°~60° because of the influence of the edged semicircular hole.

3.3.3. Case of simultaneously varied radius of an edged semicircular hole and crack length

The F_1 and F_2 values for the analytical model of Al/ Epoxy bonded dissimilar materials as shown in Figure

Table 9. Stress intensity factor of an interface crack emanating from an edged semicircular hole.

R \ a/W, F		0.003	0.017	0.033	0.100	0.200	0.300	0.400	0.500
1 mm	F_1	1.003	0.960	0.935	0.900	0.930	1.016	1.142	1.339
	F_2	0.343	0.357	0.383	0.433	0.477	0.512	0.537	0.599
5 mm	F_1	0.735	0.852	0.927	1.120	1.220	1.383	1.644	2.050
	F_2	0.221	0.316	0.383	0.522	0.589	0.634	0.668	0.706
10 mm	F_1	0.797	0.979	1.058	1.236	1.513	1.827	2.186	3.018
	F_2	0.175	0.290	0.365	0.518	0.635	0.749	0.931	1.195

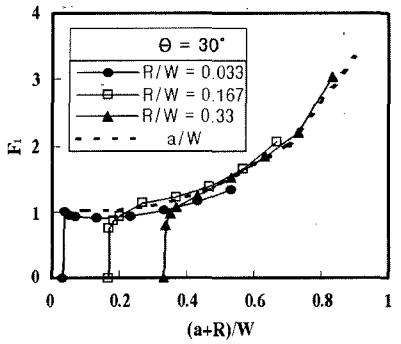

(a) Relationship between F_1 and (a+R)/W for R/W

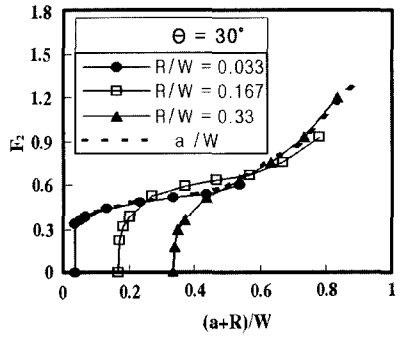

(b) Relationship between F_2 and (a+R)/W for R/W

Figure 12. Stress intensity factor for an interface crack emanating from an edged semicircular hole (θ=30).

1(b) are listed in Table 9. The stress intensity factors shown in Figure 12 were calculated when the radii of semicircular holes are R=1 mm, 5 mm and 10 mm (R/W =0,033, 0.167, 0.33), slant angle is θ=30°, and crack lengths are a=0.1 mm, 0.5 mm, 1 mm, 3 mm, 6 mm, 9 mm, 12 mm and 15 mm (a/W=0.003, 0.017, 0.033, 0.1, 0.2, 0.3, 0.4, 0.5).

Figure 12 shows the results of the numerical analysis for (a+R)/W. F_1 and F_2 are influenced by both semicircular hole radii and crack length, but they decrease when (a+R)/W>0.6 because of the influence of the semicircular hole radii and converge to stress intensity factors which have only interface cracks without holes.

4. CONCLUSIONS

The numerical results of stress intensity factors for interface cracks emanating from a centered circular hole and an edged semicircular hole by BEM are summarized as follows:

(1) In comparison with theoretical solutions and our numerical analysis by BEM for a homogeneous material and dissimilar materials with cracks, our results agree with the theoretical results within 0.1% for a homogeneous material and 0.03% for bonded dissimilar materials, respectively.

(2) The stress intensity factors for slant interfacial cracks emanating from a centered circular hole in bonded dissimilar materials are strongly influenced by the crack length when the hole radius is small, but they are strongly influenced by both the crack length and circular hole when the hole radius is large. In addition, the stress intensity factors for the crack-tip B are strongly influenced than crack-tip A by presence of the centered circular hole.

(3) The stress intensity factors for the slant interfacial crack emanating from an edged semicircular hole in bonded dissimilar materials are more strongly affected by the crack length when its radius is small, and they are strongly influenced by the edged semicircular hole when (a+R)/W < 0.6.

(4) By using the boundary element method (BEM) of numerical analysis in this study, it is possible to analyze the stress intensity factors with a high degree of accuracy and efficiency in structures composes of bonded dissimilar materials. Using these results provides a method for evaluating the strength of these materials.

ACKNOWLEDGMENT–This work was supported by the Soongsil University research fund.

REFERENCES

Bowie, O. L. (1956). Analysis of an finite plate containing radial cracks originating at the boundary of an infinite circular hole. *J. Math. Phys.*, **35,** 60–71.

Bowie, O. L. (1973). *Soultion of Plane Crack Problems by Mapping Technique.* Mechanics of Fracture (Ed. Sih G. C.). Noordhoff International Publishing Leyden, **1,** 1–55.

Chung, N. Y. (2002). Evaluation method of interface strength in bonded dissimilar materials of Al/Epoxy. *Korea Society of Mechanical Engineers(A)* **26, 11,** 2277–2286.

Chung, N. Y. and Jang, J. M. (1997). Fracture criterion of mixed mode in adhesively bonded joints of Al/Steel dissimilar materials. *Korea Society of Mechanical Engineers(A)* **21, 8,** 1322–1331.

Chung, N. Y. and Park, S. I. (2004). Detection of interfacial crack length by ultrasonic attenuation coefficients on adhesively bonded joints. *Int. J. Automotive Technology* **5, 4,** 303–309.

Chung, N. Y. and Song, C. H. (1996). Prediction of propagation path for the interface crack in bonded dissimilar materials. *Trans. Korean Society of Automotive Engineers* **4, 3,** 112–121.

Chung, N. Y., Lee, M. D. and Kang, S. K. (2000). Analyses of stress intensity factors and evaluation of fracture toughness in adhesively bonded DCB joints.

Korea Society of Mechanical Engineers(A) **24, 6,** 1517–1556.

Comninou, M. (1977). Interface crack with friction in contact zone. *J. Appl. Mech.*, **44,** 780–781.

Comninou, M. (1977). The interface crack. *J. Appl. Mech.*, **44,** 631–636.

England, F. (1965). Stress distribution in bonded dissimilar materials with cracks. *J. Appl. Mech.*, **32,** 403–410.

Erdogan, F. (1965). Stress distribution in bonded dissimilar media. *J. Appl. Mech.*, **32,** 403–410.

Erdogan, F. and Sih, G. C. (1963). On the crack extension in plate under plane loading and transverse shear. *J. Basic Eng. Trans.* **85,** 519–527.

Groth, H. (1967). Some problems of bonded anisotropic plate with cracks along the bond. *Int. J. Frac. Mech.* **3,** 253–265.

He, M. Y. and Hutchinson, J. W. (1989). Kingking of a crack out of an interface. *J. Appl. Mech.*, **56,** 270–278.

Isida, M. and Noguchi, H. (1984). Tension of a plate containing an embedded elliptical crack. *Eng. Frac. Mech.*, **20, 3,** 387–408.

Kane, J. H. (1994). *Boundary element analysis in engineering continuum mechanics.* Prentice-Hall, Inc. 161–167, New Jersy.

Kuo, A. S., Saul, S. and Levy, M. (1983). Stress intensity factors for two cracks emanating from two holes and approaching each other. *Eng. Frac. Mech.*, **17, 3,** 281–288.

Mukai, D. J., Ballarini, R. and Miller, G. R. (1990). Analysis of branched interface cracks. *J. Appl. Mech.*, **57,** 887–893.

Murakami, Y. and Nasser, S. N. (1982). Interacting dissimilar semi-elliptical surface flaws under tension and bending. *Eng. Frac. Mech.*, **16, 3,** 373–386.

Newman, J. C. (1971). An improved method of collocation for the stress analysis of cracked plate with various shaped boundaries. *NASA TA D-6373.*

Raju, I. S. (1987). Calculation of strain-energy release rates with higher order and singular finite elements. *Eng. Frac. Mech.*, **28, 3,** 251–274.

Rice, J. R. (1988). Elastic fracture mechanics concepts for interfacial cracks. *J. Appl. Mech.*, **55,** 98–103.

Rice, J. R. and Sih, G. C. (1965). Plane problems of cracks in dissimilar media. *J. Appl. Mech.*, **3,** 418–423.

Salama, M. and Hasebe, N. (1996). Stress concentration factors at an elliptical hole on the interface between bonded dissimilar half-plane under bending moment. *J. Appl. Mech.*, **63,** 7–14.

Williams, M. L. (1959). The stresses around a fault or crack in dissimilar media. *Bull. Seismol. Soc. America.* **49,** 199–204.

Woo, C. W., Wang, Y. H. and Cheung, Y. K. (1989). The mixed mode problems for the cracks emanating from a circular hole in a finite plate. *Eng. Frac. Mech.*, **32, 2,** 279–288.

Yuuki, R. and Cho, S. B. (1989). Efficient boundary element analysis of stress intensity factors for interface cracks in dissimilar materials. *Eng. Frac. Mech.*, **34, 1,** 179–188.